Bifurcations and instabilities in rotating two-layer fluids: I.f-plane

A. F. Lovegrove, I. M. Moroz, P. L. Read

Nonlinear Processes in Geophysics (2001) 8: 21–36

Nonlinear Processes in Geophysics

Bifurcations and instabilities in rotating two-layer fluids: I. f-plane

A. F. Lovegrove[1,*], **I. M. Moroz**[2], **and P. L. Read**[1]

[1]Atmospheric, Oceanic & Planetary Physics, University of Oxford, United Kingdom
[2]Mathematical Institute, University of Oxford, United Kingdom
[*]Present address: Smiths System Engineering, Guildford, UK

Received: 25 May 2000 – Revised: 17 July 2000 – Accepted: 11 August 2000

Abstract. In this paper, we show that the behaviour of weakly nonlinear waves in a 2-layer model of baroclinic instability on an f-plane with varying viscosity is determined by a single, degenerate codimension three bifurcation. In the process, we show how previous studies, using the method of multiple scales to derive evolution equations for the slowly varying amplitude of the growing wave, arise as special limits of the general evolution description. A companion study will extend the results to a β-plane.

1 Introduction

A rapidly rotating, stratified fluid with a horizontal temperature gradient, such as the atmosphere or oceans, can become unstable to small, growing perturbations. These disturbances draw their energy from the available potential energy of the fluid, which is released by "rearranging" the fluid so that it is in its state of minimum energy, with its isopycnals (lines of constant density) or isentropes as close to horizontal as possible. In the atmosphere, a consequence of this rearrangement is that warm air is transported poleward whilst cold air moves towards the equator. An instability that can produce this poleward transport of warm air is therefore able to transform the available potential energy of the fluid into kinetic energy, allowing a disturbance to grow. This form of instability is known as *baroclinic instability*.

The work presented in this paper is the first of a two-part study which aims at unifying the results of the previous multiple-scale studies of Moroz (1981) and Pedlosky (1970, 1971, 1987) of the instability of a single wave in a two-layer model of baroclinic instability on an f-plane with varying viscosity. Part II of the study extends the investigation to a β-plane. Using a spectral model of baroclinic instability Lovegrove (1998), we show that the bifurcations observed in such a model are the result of a single degenerate codimension-three bifurcation or organising centre.

Correspondence to: P. L. Read

Many cases of baroclinic instability of geophysical interest are typically found in a regime in which a small number of spatial modes can give rise to dynamics of surprising complexity. Previous studies of baroclinic flow in such regimes (e.g. Lorenz, 1962; Pedlosky, 1970, 1971; Appleby, 1982; Klein, 1990) have tended to make use of either numerical integrations of ordinary differential equations derived from a spectral expansion of the governing equations of motion, or of a multiple-scale derivation of the equations describing the interactions between a single wave and the mean flow.

While the spectral model that we consider below represents the simplest possible truncation, and which therefore has ramifications concerning comparisons with laboratory models and other physical systems, it is hoped that such a simplification will provide valuable insight into some aspects of the behaviour of these more complex and realistic models. Moreover, such highly truncated systems have long been used as paradigms for the study of weakly nonlinear baroclinic waves (e.g. see Klein, 1990, and references therein), and exhibit many of the same qualitative features as found (at least for weakly supercritical baroclinic flow) in laboratory experiments (e.g. Hide and Mason, 1975; Hart, 1979; Read et al., 1992; Früh and Read, 1997). While we have explicitly neglected interfacial Ekman layers and sidewall boundary layers (Klein and Pedlosky, 1992; Mundt et al., 1995), so as to facilitate comparison with a wide range of earlier multiple scales analyses, effects of internal friction have been incorporated in a self-consistent manner (see Section 2.3).

The theoretical investigations presented in this paper use the spectral approach, which is described in Section 2. Section 3 summarises previous multiple-scale analyses, while Section 4 describes the bifurcation structure on an f-plane. Section 5 discusses two-parameter continuations and Section 6 the organising centre. The corresponding multiple-scale derivation for the degenerate bifurcation is summarised in Section 7 and we draw our conclusions in Section 8.

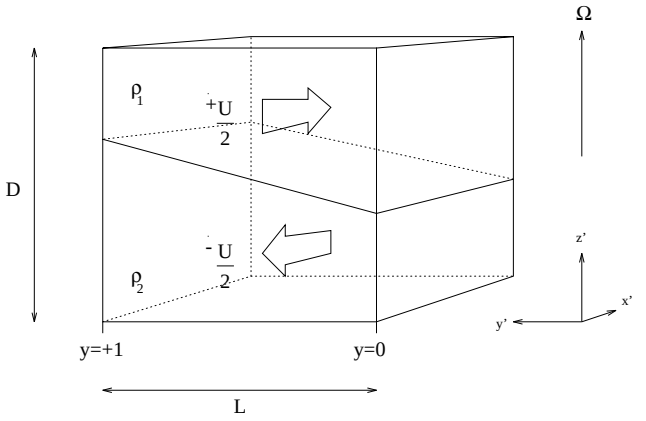

Fig. 1. The two-layer model considered in this study: comprising two immiscible fluids of densities ρ_1 and ρ_2 with $\rho_1 < \rho_2$. The fluids are in relative motion, with velocities of $+U/2$ and $-U/2$ respectively. The channel has height D, length L and is rotating at a constant angular velocity Ω.

2 The 2-layer model

The 2-layer model considered is shown schematically in Figure 1. Two superposed fluids are confined to a rotating, rectangular channel, of height D, width L and of infinite length. A Cartesian coordinate system, x', y' and z', describes, respectively, distances along the channel, across the channel and vertically. The corresponding velocities are u'_n, v'_n and w'_n, where the subscript $n = 1$ refers to the upper layer and $n = 2$ to the lower layer. The densities of the upper and lower layers are ρ_1 and ρ_2, with $\rho_2 > \rho_1$. In the absence of motion, the fluid layers have equal depths of $D/2$. The fluid is confined vertically between two horizontal planes representing a base and a lid. Dissipation is parameterised by Ekman layers on these surfaces, together with an internal diffusion term. In our analysis the kinematic viscosity within each layer is assumed to be equal, in spite of the different fluid densities.

The analysis is carried out in a reference frame that is moving with the speed, $\left(u'_1 + u'_2\right)/2$, of the mean-flow. In this frame, both the upper and lower layers appear to be in uniform motion along the channel, with velocities of $+U/2$ and $-U/2$ respectively. This choice of reference frame differs from that used in previous multiple-scale analyses of the two-layer model (e.g. Pedlosky, 1987, and references therein), where the reference frame is generally chosen to be one in which the channel itself is stationary. This new choice of reference frame does not cause any loss of generality in the model. It merely changes the apparent velocities of any waves that may form on the interface so that, for example, a wave that might be described as moving at the speed of the mean-flow, in the reference frame of previous multiple-scale analyses, will appear stationary in the present reference frame.

The various quantities in the spectral model are non-dimensional with respect to the horizontal length scale L, the vertical length scale D and the horizontal velocity scale U, a suitable advective time scale being L/U.

Non-dimensional parameters defining the state of the flow include

$$\epsilon = U/\left(f_0 L\right),$$
$$F = 2\rho_2 f_0^2 L^2/\left[\left(\rho_2 - \rho_1\right) g D\right],$$
$$\beta = L^2 \beta'/U,$$
$$r = \frac{\sqrt{2\nu f_0}L}{UD},$$

where ϵ is the Rossby number, F is the internal Froude number, β' the 'planetary' vorticity gradient, β being its dimensionless form, f_0 is the reference value of the Coriolis parameter, g is the acceleration due to gravity and r the dissipation parameter. The Rossby number measures the relative importance of inertial forces, compared with rotational forces; the internal Froude number is a ratio of rotational to buoyancy forces; β allows for a first-order variation in the background rotation with cross-channel position and r measures the strength of Ekman friction, ν being the kinematic viscosity. In this paper we set $\beta = 0$; Part II of our study will reinstate β.

A linear analysis of the full equations of motion (e.g. James, 1977) shows that two principal types of instability are possible in the two-layer model: pure baroclinic instability occurring at high rotation rates (low Rossby number); and pure Kelvin-Helmholtz instability occurring at very high Rossby number. A mixed mode instability occurs between these two extremes (King, 1979). As the present study is concerned primarily with baroclinic instability, the analysis will be restricted to regions where the Rossby number is very much less than unity ($\epsilon \ll 1$). This restriction, part of the quasigeostrophic approximation, acts as a low pass filter – preventing any high frequency waves, such as Kelvin-Helmholtz waves, from appearing in the solution to the equations of motion. Note that, in addition to the requirement that $\epsilon \ll 1$, the quasigeostrophic approximation also requires that the parameter $\beta \lesssim 1$ (see Pedlosky, 1987, for a discussion).

2.1 The governing equations

We introduce barotropic and baroclinic streamfunctions, ψ_s and ψ_d respectively, where

$$\psi_s = \left(\psi_1 + \psi_2\right)/2, \quad \psi_d = \left(\psi_1 - \psi_2\right)/2. \tag{1}$$

and define the barotropic and baroclinic velocities, U_d and U_s as

$$U_s = \left(u_1 + u_2\right)/2, \quad U_d = \left(u_1 - u_2\right)/2. \tag{2}$$

(Recall that the reference frame was chosen so that $u'_1 = U/2$ and $u'_2 = -U/2$, which implies that $U_d = 1/2$ and $U_s = 0$.) In this new form, the governing quasigeostrophic potential vorticity equations are

$$\frac{\partial}{\partial t}\nabla^2\psi_s + \beta\frac{\partial \psi_s}{\partial x} + J\left(\psi_s, \nabla^2\psi_s\right) + J\left(\psi_d, \nabla^2\psi_d\right) = -r\nabla^2\psi_s + r^2\epsilon\nabla^4\psi_s, \tag{3}$$

$$\frac{\partial}{\partial t}\left(\nabla^2 - 2F\right)\psi_d + \beta\frac{\partial \psi_d}{\partial x} + J\left(\psi_s, \nabla^2\psi_d\right) + J\left(\psi_d, \nabla^2\psi_s\right) + 2FJ\left(\psi_d, \psi_s\right) = -r\nabla^2\psi_d + r^2\epsilon\nabla^2\left(\nabla^2 - 2F\right)\psi_d, \quad (4)$$

where J is the usual Jacobian operator. In the above formulation we have ignored the effects of interfacial Ekman friction, since our objective here is to place the earlier multiple-scale studies (in which such friction was absent) in context using the spectral model. For the same reason, we also ignored sidewall boundary layers. As pointed out e.g. by Hart (1986), Mundt et al. (1995), and Polvani and Pedlosky (1988), however, the neglect of such factors can significantly influence the subsequent dynamics.

2.2 Spectral expansion

Solutions are sought in which the streamfunctions are expanded in series of Fourier modes:

$$\psi_{s,d} = \sum_{m=1}^{M} X_m^{s,d}\cos l_m y + \sum_{\substack{n=-N \\ n\neq 0}}^{N}\sum_{m=1}^{M} W_{nm}^{s,d}\exp\left(ik_n x\right)\sin l_n y, \quad (5)$$

where $W_{-mn}^{s,d} = \left(W_{mn}^{s,d}\right)^*$, $k_{-m} = -k_m$, and the asterisk denotes complex conjugation. The first term on the right hand side of equation (5) is the *mean flow correction* term; the second term is the *wave term*. Equations (3) and (4) are solved subject to boundary conditions which require the sidewalls to be impermeable, so that the meridional velocity vanishes at the sidewalls (see Pedlosky, 1987):

$$\frac{\partial \psi_{s,d}}{\partial x} = 0 \quad \text{on} \quad y = 0, 1. \quad (6)$$

To ensure the absence of unspecified energy flux through the sidewalls (Phillips, 1954), we also require:

$$\lim_{X\to\infty}\frac{1}{2X}\int_{-X}^{X}\frac{\partial^2\psi_{s,d}}{\partial y\partial t}\,dx = 0 \quad \text{on} \quad y = 0, 1. \quad (7)$$

In addition, the channel is assumed to be periodic in the x-direction. i.e.

$$\psi_{s,d}\left(x\right) = \psi_{s,d}\left(x + X_T\right), \quad (8)$$

where X_T is the spatial period of the flow. These boundary conditions require the azimuthal and meridional wavenumbers to be $k_n = 2n\pi/\alpha$ and $l_m = m\pi$, where α is the aspect ratio (i.e. the ratio of cross-channel length to along-channel length), which has been set to 6 for this study as this is approximately the value for a typical experimental annulus system.

2.3 Dissipation parameterisation

The principal dissipation terms in equations (3) and (4) are the Ekman layer parameterisations (the first terms on the right hand side), although an internal dissipation term, parameterised by a potential vorticity diffusion (Lewis, 1992), is also included. This second form of diffusion is often included in numerical models, its purpose being to dissipate energy that is transferred to high wavenumbers through wave interactions. For example, in a spectral model two waves, k_2 and k_1, can interact to produce waves with wavenumbers $(k_2 - k_1)$ and $(k_2 + k_1)$. Energy is therefore transferred from waves k_2 and k_1 to these product waves. If the truncation of the spectral model is such that the product wave $(k_2 + k_1)$ is not represented, however, then the energy associated with this wave will be aliased back into lower wavenumbers, close to the truncation limit. The product wave is therefore a spurious energy source.

A dissipation term that varies as ∇^4 is more scale-selective than a dissipation term that varies as ∇^2 and therefore has a stronger effect on shorter waves than the latter. As the purpose of the internal dissipation is to remove the spurious energy source, it is chosen to vary as ∇^4. This extra dissipation term differs slightly from the simple ∇^2 dissipation term usually used in studies of the two-layer model (e.g. Pedlosky, 1970), in which the dissipation is provided by Ekman layers on the endwalls alone.

2.4 The truncated system

For this study, the truncation of equations (5) was chosen to be at $M = 1$, and $N = 1$ so that only the first non-constant terms in the expansion (5) were considered. This is the simplest possible truncation, and describes the interaction between one azimuthal wave and the mean flow. While no attempt is made to justify this truncation physically, it is hoped that such a simple model will provide a valuable first step towards the bifurcation analysis of more complex models, involving wave-wave interactions, although we recognise that our results may display some sensitivity to the level of truncation (Klein and Pedlosky, 1986). Several studies have investigated the effects of different levels of truncation, and their principal conclusions are that, while the inclusion of further wave modes can substantially alter the behaviour of the system (Curry, 1978), altering the number of modes in the mean-flow correction does not (Booty et al., 1982).

Substituting (5) into (3) and (4), we obtain the following set of coupled, ordinary differential equations:

$$\begin{aligned}
\dot{A_s} &= -\Delta_s A_s + \beta_s B_s - \left(\nu_s + \gamma_s X_d\right) B_d, \\
\dot{B_s} &= -\Delta_s B_s - \beta_s A_s + \left(\nu_s + \gamma_s X_d\right) A_d, \\
\dot{A_d} &= -\Delta_d A_d + \beta_d B_d - \left(\nu_d + \gamma_d X_d\right) B_s, \\
\dot{B_d} &= -\Delta_d B_d - \beta_d A_d + \left(\nu_d + \gamma_d X_d\right) A_s, \\
\dot{X_d} &= -\bar{\Delta} X_d + \bar{\gamma}\left(A_s B_d - B_s A_d\right),
\end{aligned} \quad (9)$$

where the dot represents differentiation with respect to time, $A_{s,d} = \mathrm{Re}\left(W_{11}^{s,d}\right)$, and $B_{s,d} = \mathrm{Im}\left(W_{11}^{s,d}\right)$. The various

coefficients are given in Appendix A. The equation for $\dot{X}_s$ has been omitted since it describes the simple exponential decay of X_s. The equilibrium value of X_s is therefore always zero and is consequently of little interest for this study.

3 Multiple-scale studies

In multiple-scale analyses of the two-layer model (e.g. see Pedlosky, 1970, 1971; Moroz, 1981) the quasigeostrophic potential vorticity equations are usually written in terms of streamfunctions for layer 1 and layer 2. The total streamfunction for each layer is then

$$\psi_n = \psi_n^{(0)} + \phi_n, \; n = 1, 2, \tag{10}$$

where $\psi_n^{(0)} = -u_n y$ is the streamfunction for the basic state and ϕ_n represents a perturbation to the basic state. One seeks solutions to the quasigeostrophic potential vorticity equations in the form

$$\phi_1 = \mathrm{Re} A e^{ik(x-ct)} \sin ly, \quad \phi_2 = \mathrm{Re} \gamma A e^{ik(x-ct)} \sin ly \tag{11}$$

where l is the cross-channel wavenumber, k is the along-channel wavenumber of the disturbance, A is the amplitude of the wave in the upper layer, and γA is the amplitude of the wave in the lower layer, γ being a (possibly) complex parameter; $c = c_r + ic_i$, where c_r represents the along-channel wave speed and c_i describes the growth (or decay) rate of the wave amplitude. One of the model parameters (usually the vertical shear, U_d, or the Froude number, F) is chosen as the principal bifurcation parameter, (11) is then substituted into the quasigeostrophic potential vorticity equations and solved for the case of marginal stability, i.e. when $c_i = 0$. Small perturbations, δ, from the state of marginal stability are then studied by seeking a series solution of the form

$$\phi_n = |\delta|^{\frac{1}{2}} \phi_n^{(0)} + |\delta| \phi_n^{(1)} + |\delta|^{\frac{3}{2}} \phi_n^{(2)} + \ldots. \tag{12}$$

A new slow timescale, $T = \delta^{\frac{1}{2}} t$, is also introduced, although other scalings are possible. Other parameters, such as β or r, are also scaled as powers of the supercriticality parameter. Equating successive powers of δ and removing secular terms then leads to a set of ordinary differential equations governing the evolution of the amplitude of the growing disturbance. Since δ is assumed to be small, this places restrictions on the size of any other parameters (such as β and r) that may have been scaled on δ. The scaling of β and r must therefore be varied in order to examine different regions of the (r, β) parameter plane, giving rise to different multiple-scale approximations. These various approximations are summarised in Table 1 and will now be discussed.

3.1 Instability on an f-plane

3.1.1 Strongly dissipative systems: r = O(1)

Pedlosky (1970) performed a multiple-scale analysis of slowly-varying wave-trains in a strongly dissipative two-layer system. The bifurcation parameter was the vertical shear, U_d, and δ was given by $U_d - U_c = \delta$ where $\delta \ll U_c$, and U_c, the critical value of U_d for which a shear-flow was stable for all $U_d < U_c$, was given by

$$U_c = \frac{rK}{k_n \left(2F - K^2\right)^{1/2}}. \tag{13}$$

The corresponding value for c_r was found to be $c_r = U_s = (u_1 + u_2)/2$, which is independent of the wavenumber k_n. The f-plane model is therefore non-dispersive.[1] Defining a strongly dissipative system to be one in which $r \approx \mathcal{O}(1)$, Pedlosky (1970) showed that the evolving wave amplitude satisfies

$$\dot{A} = A - AV, \quad V = |A|^2, \tag{14}$$

where the dot here denotes differentiation with respect to the slow time, $T = \delta t$, A is the amplitude of the wave present on the interface between the two fluids and V is the mean-flow correction. The details of the coefficients in the equation have been omitted, but may be found in Pedlosky (1970) and Moroz (1981). $A = 0$ is always a fixed point of equation (14), and corresponds to the axisymmetric flows observed in rotating annulus experiments such as those of Früh and Read (1997).

As U_d increases, the trivial solution loses stability via a pitchfork bifurcation to a wave, travelling at the mean-flow speed on the fluid interface, and corresponds to the steady wave flows seen in rotating annulus experiments. The final state, in which the equilibrium wave has achieved its maximum amplitude, is independent of the initial state of the system (apart from its phase).

3.1.2 Inviscid systems: r = 0

Pedlosky (1970) also derived the multiple-scale approximation for the inviscid system, $r = 0$, on an f-plane. Here, the bifurcation parameter was taken to be F, with the supercriticality parameter $\mathcal{F}$ defined by $F - F_c = \mathcal{F}$, where $\mathcal{F} \ll \mathrm{F_c}$, and $F_c = K^2/2$ is the critical Froude number.

The multiple-scale approximation yields

$$\ddot{A} = A - AV, \quad \dot{V} = |\dot{A}|^2. \tag{15}$$

Once again, the trivial solution is always a fixed point of the equations. However, in the inviscid system, the trivial solution loses stability, not to a stationary wave but to a modulated wave that varies with time. Pedlosky does not comment on the nature of the bifurcation from the trivial solution to the oscillatory motion.

3.1.3 Weakly dissipative systems: r = O($\delta^{1/2}$)

Pedlosky (1971) extended his multiple-scale analysis to the weakly dissipative regime, again using $\mathcal{F}$ as the supercriticality parameter, and taking $r \approx \mathcal{O}\left(\mathcal{F}^{\frac{1}{2}}\right)$. In this case he

[1] Recall that the spectral model was analysed in a reference frame moving at the speed of the mean-flow. Consequently, in this frame, the f-plane waves would appear to be stationary.

	$\beta = 0$	$\beta = \mathcal{O}\left(\mathcal{F}^{1/2}\right)$	$\beta = \mathcal{O}(1)$
$r = 0$	$\ddot{A} = A - AV$ $\dot{V} = \|\dot{A}\|^2$ $T = \|\mathcal{F}\|^{1/2}t$ Pedlosky (1970)	$\ddot{A} = A - c\dot{A} - AV$ $\dot{V} = \|\dot{A}\|^2$ $T = \|\mathcal{F}\|^{1/2}t$ Moroz (1981)	$\ddot{A} = A - AV$ $V = \|\dot{A}\|^2$ $T = \|\mathcal{F}\|^{1/2}t$ Pedlosky (1970)
$r = \mathcal{O}\left(\mathcal{F}^{1/2}\right)$	$\ddot{A} = A - \dot{A} - AV$ $\dot{V} = \|\dot{A}\|^2 + \|A\|^2 - V$ $T = \|\mathcal{F}\|^{1/2}t$ Pedlosky (1971) Gibbon & McGuinness (1982)	$\ddot{A} = cA - c\dot{A} - AV$ $\dot{V} = \|\dot{A}\|^2 + \|A\|^2 - V$ $T = \|\mathcal{F}\|^{1/2}t$ Fowler et al. (1982)	$\dot{A} = A - AV$ $\dot{V} = \|A\|^2$ $T = \|\mathcal{F}\|t$ Moroz (1981)
$r = \mathcal{O}(1)$	$\dot{A} = A - AV$ $V = \|A\|^2$ $T = \|\delta\|t$ Pedlosky (1970)	$\dot{A} = cA - AV$ $V = \|A\|^2$ $T = \|\delta\|t$ Moroz (1981)	$\dot{A} = cA - cAV$ $V = \|A\|^2$ $T = \|\delta\|t$ Romea (1977)

Table 1. Summary of previous multiple-scale approximations, showing their location on the $[r, \beta]$-plane. A is the amplitude of the interfacial wave, V is the mean-flow correction. c denotes a complex coefficient, and following Moroz (1981), the details of the coefficients have been omitted. The slow-time is given by T, while t denotes the 'original' unscaled time. (Table after Moroz, 1981.) The supercriticality parameters, δ and $\mathcal{F}$ are defined in the text.

obtained

$$\ddot{A} = A - \dot{A} - AV,$$
$$\dot{V} + V = |\dot{A}|^2 + |A|. \tag{16}$$

Gibbon and McGuinness (1982) and Pedlosky and Frenzen (1980) later showed independently that equations (16) reduce to the equations originally derived by Lorenz (1963) to describe two-dimensional convection in a horizontal layer of fluid heated from below:

$$\dot{X} = -\sigma X + \sigma Y,$$
$$\dot{Y} = RX - Y - XZ, \tag{17}$$
$$\dot{Z} = -bZ + XY,$$

where R is the Rayleigh number, σ is the Prandtl number of the fluid, and b is the aspect ratio of the system. In contrast to the simple bifurcations present for the strongly dissipative and the inviscid systems, the Lorenz equations exhibit a large number of different bifurcations, leading to complicated behaviour (e.g. Sparrow, 1982). This raises two main questions. Firstly, how are the bifurcations in the different multiple-scale approximations related to one another? Secondly, where do these bifurcations "come from"?

The spectral approach leads to a single set of spectral amplitude equations describing the behaviour of the two-layer model over the entire (r, β)-plane, and should therefore be capable of reproducing all the different forms of behaviour described by the various multiple-scale approximations – if the two approaches are to be consistent. A study of the spectral amplitude equations should therefore reveal the mechanisms by which one multiple-scale approximation "blends" into a neighbouring approximation. The differences between the mechanisms involved in inviscid and viscous bifurcations will also be discussed. More recent results describing the effects of symmetry on different bifurcations have been reported (see Lovegrove, 1998, and references therein). The present study will therefore try to exploit such results to explain the differences observed between the behaviour of the two-layer model on an f-plane and (in Part II of the study) on a β-plane. It is also possible to do a more detailed investigation of the bifurcations in the two-layer model than has been possible previously. It is hoped that the net result of this investigation will be to provide a coherent, global account of the origins of the bifurcations in the two-layer model which, in the process, draws together the different multiple-scale approximations and places them in context.

4 Bifurcations on an f-plane

We now study the bifurcations of the spectral amplitude equations (9) when $\beta = 0$, for both a strongly and a weakly dissipative system, using standard techniques of numerical solution continuation and numerical integration. To perform this analysis, the underlying symmetry of the spectral amplitude equations must be determined by defining the action of the $O(2)$ symmetry group on the space of the spectral amplitude equations and by showing that they are equivariant with respect to this action.

It is possible to define the action of the symmetry group $O(2)$ on the space of the full complex spectral amplitude equations as

$$\begin{aligned} &\text{a rotation} \quad s : (X, Y) \to \left(Xe^{i\eta}, Ye^{i\eta}\right), \\ &\text{a reflection} \quad \rho : (X, Y) \to \pm\left(X^*, Y^*\right), \end{aligned} \tag{18}$$

where X and Y are complex. Any set of equations of the form $\dot{\boldsymbol{x}} = f(\boldsymbol{x})$ which satisfies the following equivariance relations

$$f(s\boldsymbol{x}) = sf(\boldsymbol{x}), \quad f(\rho\boldsymbol{x}) = \rho f(\boldsymbol{x}) \tag{19}$$

has the following properties: (i) under the action of s, any solution $\boldsymbol{x}_0$ of the original set of equations may be multiplied by a factor $e^{i\eta}$ to obtain a new solution to the equations; and (ii) under the action of ρ, the complex conjugate of any solution of the original set of equations is also a solution to the equations.

Physically, the action of s may be thought of as representing the along-channel symmetry of the two-layer model, the angle η representing the spatial phase, ϕ, of the solution. Equivariance under the action of s means, therefore, that there is no preferred along-channel position for a stationary wave to form on the interface; any wave is equivalent to another, up to a translation along the channel. As shown below, ϕ is constant on an f-plane. Equivariance under the action of ρ indicates that any wave may be reflected in a plane cutting across the channel to give another solution to the equations.

The f-plane spectral equations are equivariant under the action of both s and ρ and therefore they possess $O(2)$ symmetry.

We show that the spectral amplitude equations are capable of reproducing the behaviour of the strongly dissipative and the weakly dissipative multiple-scale approximations of Pedlosky (1970, 1971). Furthermore, examining the bifurcations of the spectral amplitude equations in the two-dimensional (r, F)-parameter plane will allow a quantitative boundary to be placed on the range of validity of both the strongly dissipative and the weakly dissipative multiple-scale approximations. The principal bifurcations of the spectral amplitude equations will be seen to converge as $r \to 0$, meeting at a degenerate bifurcation, or *organising centre*, on the inviscid f-plane axis which has a codimension of at least two. To examine the structure of the organising centre, we perform an *unfolding* close to the organising centre so as to preserve the $O(2)$ symmetry. To third order, this unfolding is equivalent to the Lorenz equations, indicating that Lorenz-like behaviour arises naturally as a consequence of the organising centre on the inviscid f-plane axis. Furthermore, it will be shown that, as r increases, the fourth-order contributions to the unfolding become important. It is the presence of these additional terms which allow the spectral amplitude equations to capture the dynamics of both the strongly and the weakly dissipative multiple-scale approximations. The unfolding of the organising centre will then give rise to the set of equations (15), derived by Pedlosky (1970) for the case of an inviscid f-plane.

4.1 One-parameter continuations

4.1.1 The spectral amplitude equations on an f-plane

The bifurcation analyses for the spectral equations (9) were performed at two values of r, the dissipation parameter: $r = 0.2$ (representing a strongly dissipative system) and $r = 0.02$ (representing a weakly dissipative system). The choice of these values of r will be justified later (see Section 5).

The Froude number, F, was chosen to be the bifurcation parameter for these analyses, since this was the control parameter chosen by Pedlosky (1971) in his analysis of the weakly dissipative system. F is also a convenient control parameter for experiments since changing the Froude number, whilst holding r at a relatively constant value, is straightforward to realise in a laboratory setting, thereby allowing an easy comparison between theory and experiment. For both of these analyses, the Rossby number, ϵ, was held fixed at a value of $\epsilon = 0.05$ for consistency with the quasigeostrophic approximation (i.e. requiring $\epsilon \ll 1$). The mean-flow parameters U_s and U_d were taken to be 0 and 0.5 respectively, corresponding to the situation in which the two fluid layers are moving with equal and opposite velocities (so that $u_1 = +0.5$ and $u_2 = -0.5$).

In order to simplify the bifurcation analyses, the equations (9) were written in their complex form:

$$\begin{aligned} \dot{X} &= -\Delta_s X + \left(1 + \frac{\gamma_s}{\nu_s} Z\right) Y, \\ \dot{Y} &= -\Delta_d Y + \nu_s \left(\nu_d + \gamma_d Z\right) X, \\ \dot{Z} &= -\bar{\Delta} Z - \frac{\bar{\gamma}}{2\nu_s}\left(XY^* + YX^*\right), \end{aligned} \tag{20}$$

where β has been set to zero, and

$$(X, Y, Z) = \left(A_s + iB_s, -i\nu_s\left(A_d + iB_d\right), X_d\right). \tag{21}$$

Note that, in these equations, the time is not a slow time as in the multiple-scale approximations of Section 3 and that none of the parameters have been assumed to be small.

It can be seen that the trivial solution, $(X, Y, Z) = (0, 0, 0)$, representing a situation in which the interface between the two fluid layers is flat, is always a fixed point of equations (20). This trivial solution will lose stability when the real

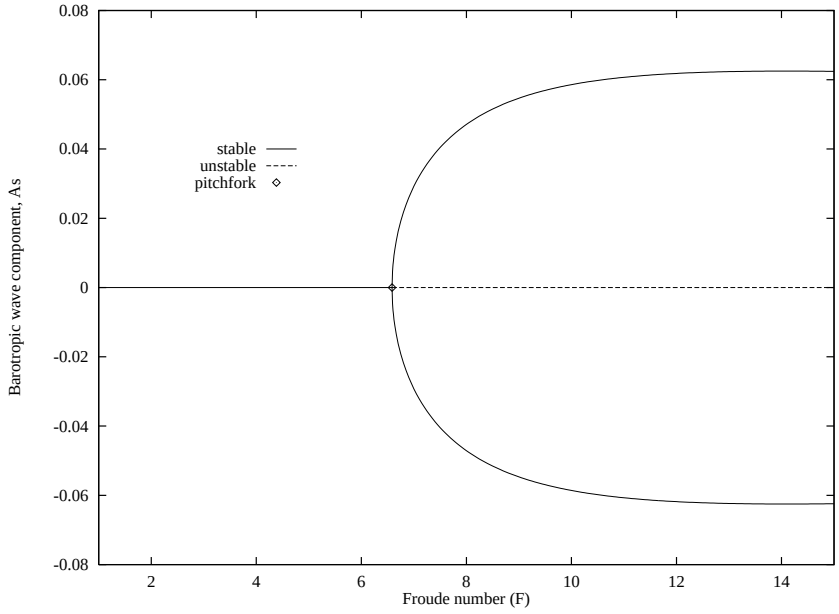

Fig. 2. Bifurcation diagram for the barotropic wave component, A_s, showing the effect of increasing the Froude number at $r = 0.2$. The trivial solution lost stability to a stationary wave in a pitchfork bifurcation at $F = 6.59$.

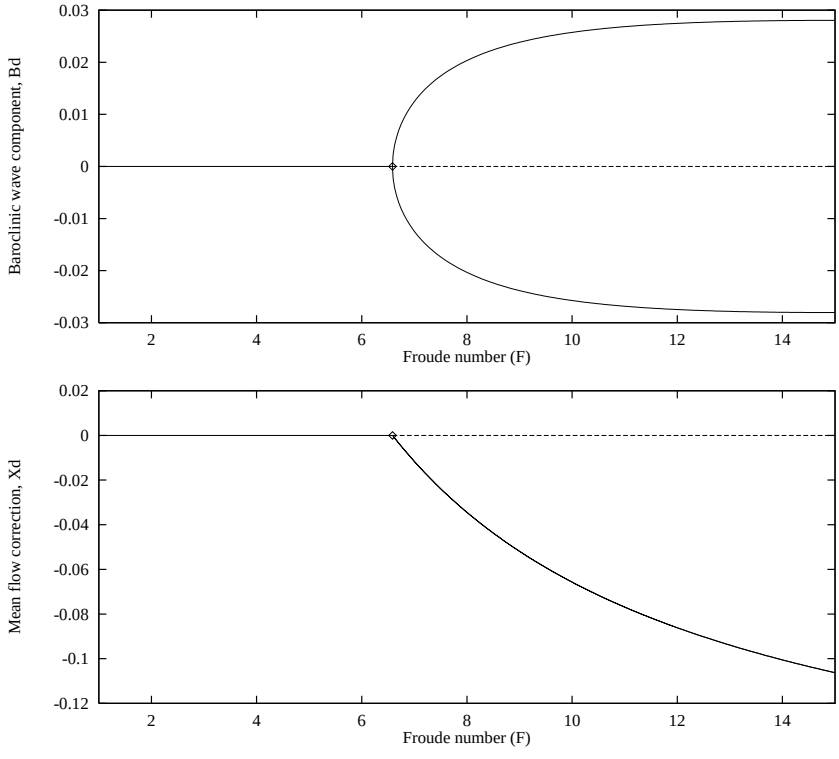

Fig. 3. Bifurcation diagrams showing the effect of increasing F at $r = 0.2$ for **(a)** the baroclinic wave component, B_d, and **(b)** the mean-flow correction X_d. The key is the same as that in Figure 2.

part of any eigenvalue λ_j of the Jacobian matrix of linearisation for small perturbations becomes positive, where

$$\begin{aligned} &\lambda_{1,2}^2 + (\Delta_s + \Delta_d)\,\lambda_{1,2} + \Delta_s\Delta_d - \nu_s\nu_d = 0, \\ &\lambda_{3,4}^2 + (\Delta_s + \Delta_d)\,\lambda_{3,4} + \Delta_s\Delta_d - \nu_s\nu_d = 0, \\ &\lambda_5 = -\bar{\Delta}. \end{aligned} \tag{22}$$

The repeated eigenvalues result from the fact that X, Y and Z are complex variables. Since $\bar{\Delta}$ is directly proportional to r, $\lambda_5 < 0$ for all nonzero values of r and z is a stable manifold. It can also be seen that, at $\Delta_s\Delta_d = \nu_s\nu_d$, two real eigenvalues λ_1 and λ_3 pass through zero and the trivial solution loses stability to a wave-like disturbance on the interface. Since the two eigenvalues involved in this bifurcation are real, the bifurcating solution does not vary with time and so represents a stationary wave. The remaining eigenvalues, λ_2 and λ_4, remain real and negative.

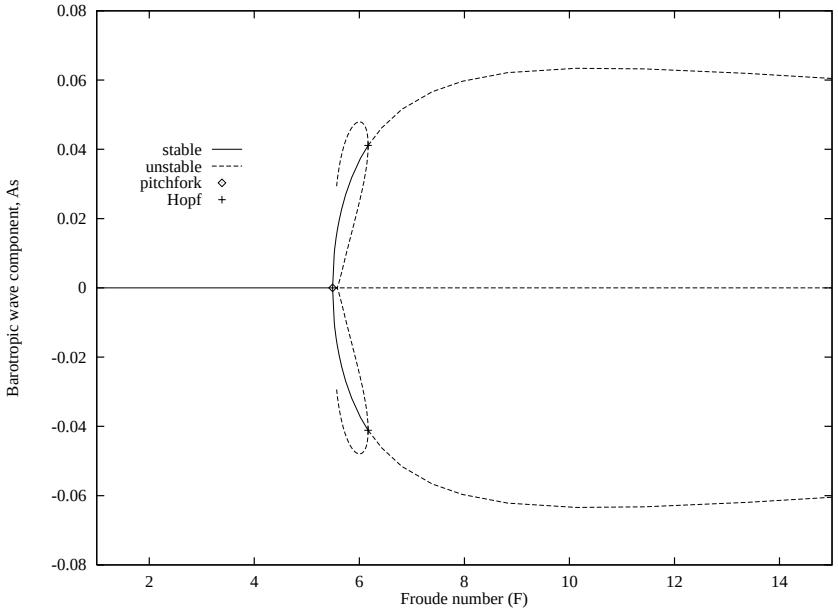

Fig. 4. Bifurcation diagram showing the effect of increasing the Froude number at $r = 0.02$. The trivial solution lost stability to a stationary wave at $F = 5.49$. The stationary wave subsequently became unstable to an unstable periodic orbit in a subcritical Hopf bifurcation at $F = 6.17$. Both the maximum and the minimum amplitudes of this orbit are shown.

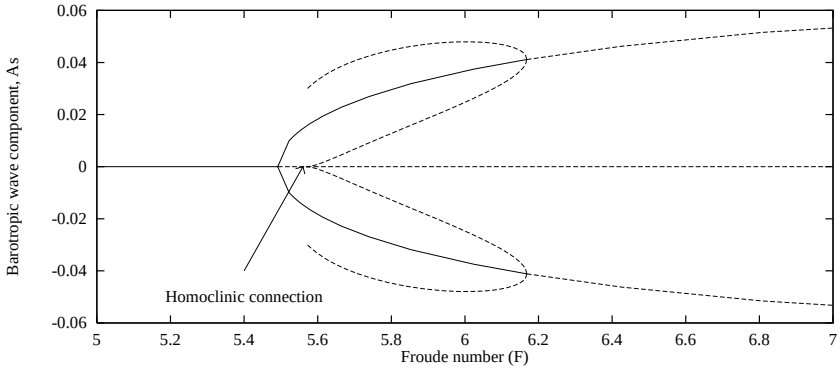

Fig. 5. Enlargement of Figure 4. Note their close approach to the unstable trivial solution at $F = 5.56$.

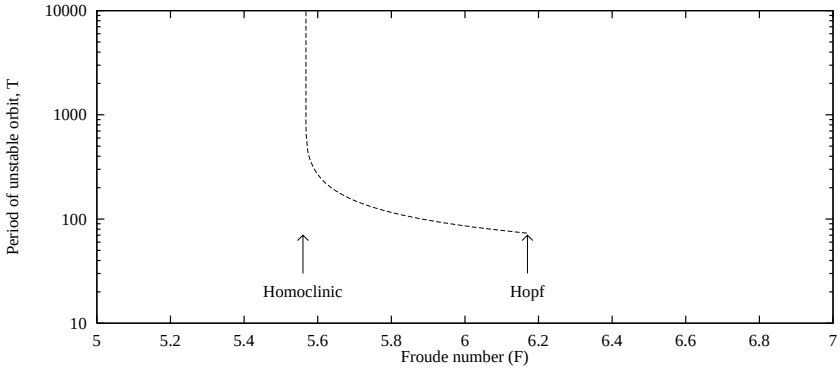

Fig. 6. Period of the unstable orbit born in the subcritical Hopf bifurcation at $F = 6.17$. Observe that the period becomes infinite as the unstable orbit approaches the trivial solution at $F = 5.56$.

4.2 Bifurcations in a strongly dissipative system ($r = 0.2$)

4.2.1 Solution continuation

Solution continuation was made using the numerical continuation software AUTO86 by Doedel (1981) and Doedel and Kernevez (1986). Unfortunately AUTO86 is unable to cope with the situation in which two real eigenvalues become zero simultaneously. At the time this work was undertaken, AUTO86 was the only facility available to us, and so we had to adopt the procedures outlined here. In order to perform numerical solution continuations, therefore, the variables X and Y were taken to be real, and so only one eigenvalue passes through zero in the initial bifurcation. This will be justified later in Section 4.4 and gives rise to

$$\begin{aligned} \dot{A}_s &= -\Delta_s X + (\nu_s + \gamma_s Z)\, B_d, \\ \dot{B}_d &= -\Delta_d B_d + (\nu_d + \gamma_d Z)\, A_s, \\ \dot{Z} &= -\bar{\Delta} Z - \bar{\gamma}\, (A_s B_d)\,. \end{aligned} \tag{23}$$

The results of this solution continuation are summarised in the form of a bifurcation diagram in Figure 2, showing the

barotropic wave component, A_s, as a function of the Froude number. The initial point on the solution curve was taken to be the trivial solution at $F = 1.0$. Increasing the Froude number causes the stable axisymmetric flow to become unstable to a stable, stationary wave in a pitchfork bifurcation at $F = F_{\rm pf} = 6.59$. Since the variables are restricted to being real, two stationary wave solutions are actually created in the pitchfork bifurcation and these are shown as two nontrivial branches in Figure 2. The fact that there *are* two solutions results from the symmetry of equations (23) under reflection $(A_s, B_d) \rightarrow -(A_s, B_d)$, which will be discussed in more detail in Section 4.4. The amplitude of the equilibrium stationary wave grows as F increases. The corresponding bifurcation diagrams for the baroclinic wave, B_d, and the mean-flow correction, X_d, are shown in Figure 3.

4.2.2 Numerical integration

The solution continuation revealed that there were only two possible solutions to the spectral amplitude equations in the strongly dissipative regime: the trivial solution, and a stationary wave solution. These two solutions were verified by initial-value numerical integrations of the full spectral amplitude equations (20), in which B_s and A_d, the imaginary parts of X and Y, were always set to zero initially to reflect the same assumption used in the solution continuation; namely, that X and Y were real.

Thus for $r = 0.2$, the restricted set of spectral amplitude equations (23) reproduces the simple pitchfork bifurcation encountered in the Landau-Stuart equation, derived by Pedlosky (1970) as the multiple-scale approximation to behaviour in a strongly dissipative two-layer model.

4.3 Bifurcations in a weakly dissipative system ($r = 0.02$)

4.3.1 Solution continuation

As in the previous section, the numerical solution continuation in the weakly dissipative system was performed on the restricted set of equations (23) in order to allow AUTO86 to proceed past the initial bifurcation. The dissipation parameter was fixed at $r = 0.02$ and, once again, the results are summarised in the form of a bifurcation diagram for the barotropic wave component, A_s, in Figure 4.

The solution continuation was initialised on the trivial solution at $F = 1$. As in the strongly dissipative system, increasing F caused the axisymmetric flow to become unstable to a stable stationary wave in a pitchfork bifurcation, this time at the slightly lower value of $F_{\rm pf} = 5.49$. In this case, however, the stationary wave underwent a Hopf bifurcation at $F = 6.17$. Using AUTO86, we were able to switch solution branches and show that this Hopf bifurcation was subcritical, which immediately raised a question as to the origin of the unstable orbit involved in the Hopf bifurcation. Using AUTO86 to trace out the branch of periodic orbits, the amplitude of the unstable periodic orbit was found to increase as F decreased. At $F = 5.56$, the amplitude of the periodic orbit had become so large that it passed through the fixed point on the axis, denoting the original (now unstable) trivial solution. This can be observed as the close approach of the branch of unstable periodic orbits to the trivial solution in Figure 4 and

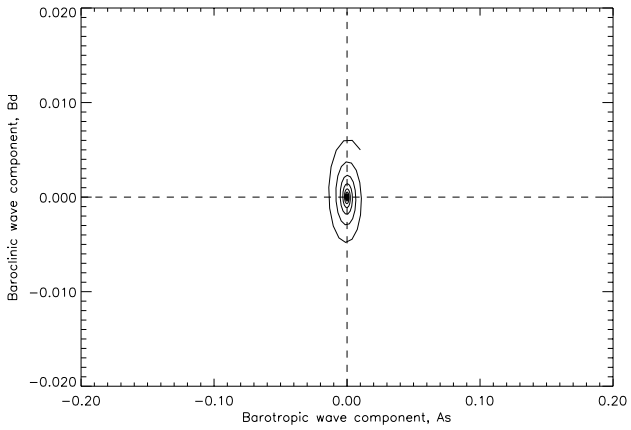

(a) $F = 4.0$

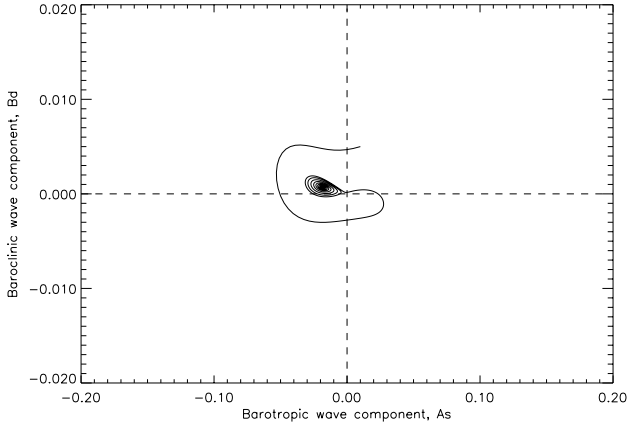

(b) $F = 5.5$

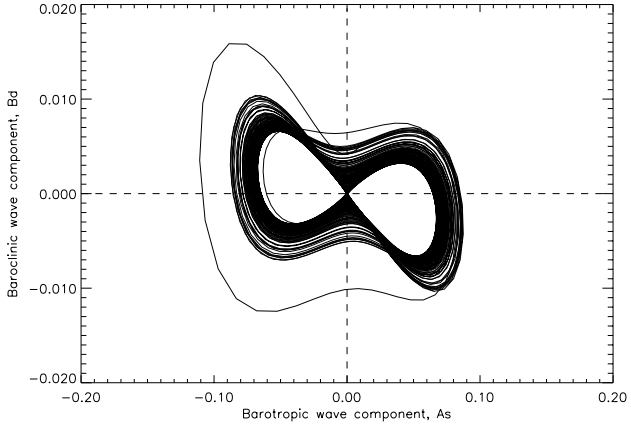

(c) $F = 6.16$

Fig. 7. Three initial value numerical integrations performed in the weakly dissipative regime at $r = 0.02$. **(a)** shows the stable trivial solution at $F = 4.0$. **(b)** shows the stable fixed point, corresponding to a stationary wave at $F = 5.5$. **(c)** shows the strange attractor at $F = 6.16$.

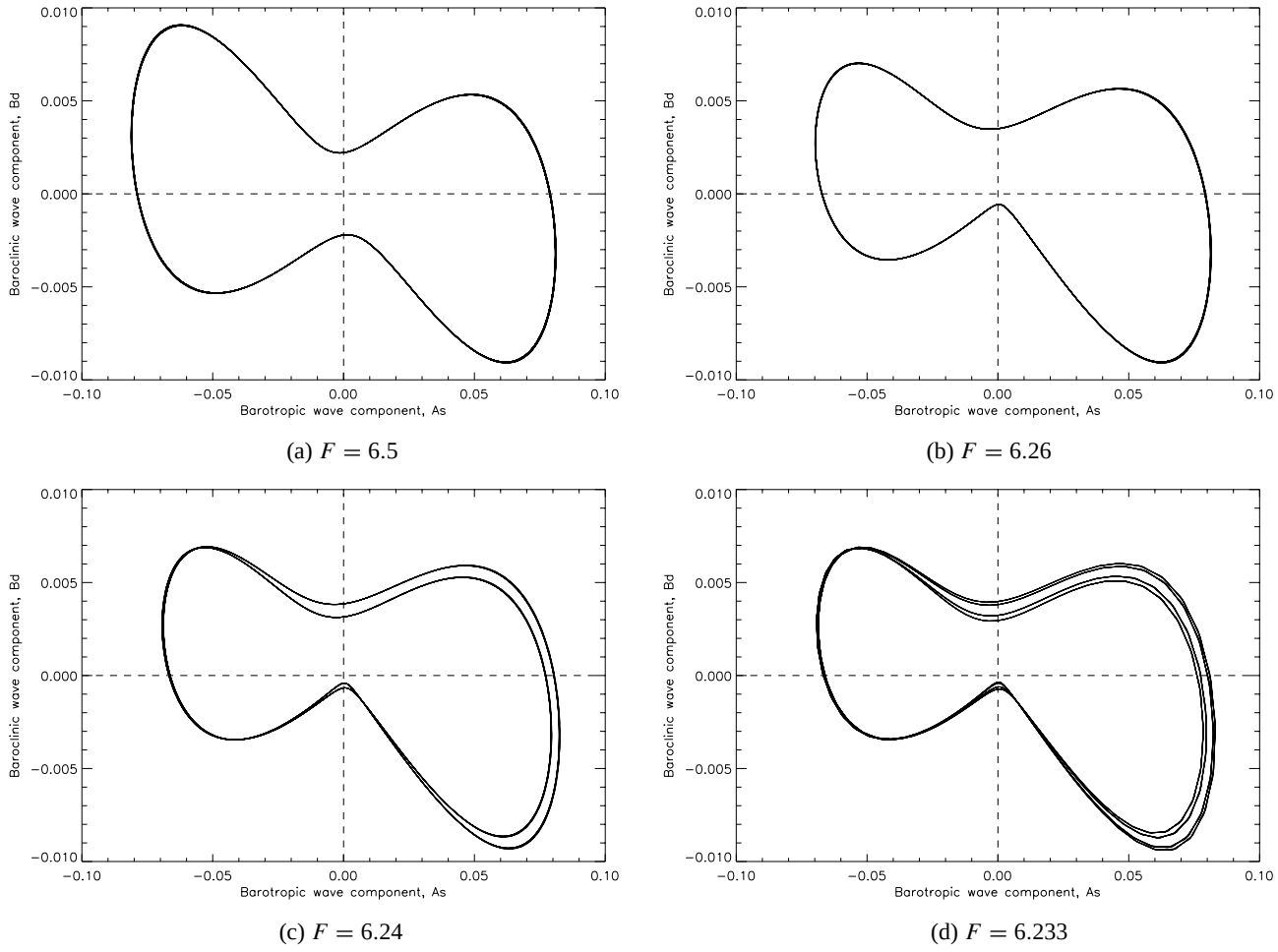

(a) $F = 6.5$ (b) $F = 6.26$

(c) $F = 6.24$ (d) $F = 6.233$

Fig. 8. A series of numerical integrations performed at $r = 0.02$. **(a)** shows the existence of a stable symmetric orbit at $F = 6.5$. **(b)** shows that the symmetric orbit was replaced by an asymmetric orbit at $F = 6.26$. This orbit subsequently period-doubles to produce **(c)** a period-2 orbit at $F = 6.24$ and **(d)** a period-4 orbit at $F = 6.233$.

Figure 5.

The period of this unstable orbit was computed as a function of F and was found to increase rapidly as $F \to 5.56$, suggesting that the unstable orbit was created in a homoclinic bifurcation at $F = 5.56$. This is similar to the situation encountered in the Lorenz equations (17) at $R = 13.96$. It will be seen in Section 4.4, however, that there is a crucial difference between the two cases.

4.3.2 Numerical integrations

The first set of integrations, shown projected onto the (A_s, B_d)-plane in Figure 7, illustrate the transition to chaos. Note that these integrations all contain transient behaviour. Figure 7 shows that, for $F < F_{\rm pf} = 5.49$, the trivial solution was stable (Figure 7a). As F was increased through $F_{\rm pf}$ a stable fixed point appeared (Figure 7b), followed by the creation of a strange attractor giving rise to chaotic behaviour at $F = 6.16$ (Figure 7a). Note that, as in the Lorenz equations, the strange attractor was created before the subcritical Hopf bifurcation at $F = 6.17$ was reached.

A second set of integrations, shown in Figure 8, illustrates the behaviour of the spectral amplitude equations at higher values of the Froude number. A symmetric periodic orbit was found to exist for all values of $F > 6.4$ (Figure 8a). Decreasing F caused this symmetric orbit to be replaced by an asymmetric orbit (Figure 8b) in a symmetry-breaking bifurcation and then to undergo a series of period doubling bifurcations. The first two of these are shown in Figures 8c and 8d.

Thus when $r = 0.02$, the restricted set of spectral amplitude equations can reproduce the Lorenz-like behaviour of the weakly dissipative multiple-scale approximation derived by Pedlosky for a weakly-dissipative two-layer model. We next generalise these results to the full, complex, spectral amplitude equations (20).

4.4 Generalisation to complex behaviour

Although, in the restricted spectral amplitude equations (23), the initial bifurcation from the trivial solution took the form of a pitchfork bifurcation, in the full complex spectral ampli-

tude equations (20), the initial bifurcation occurred when *two* real eigenvalues passed through zero. Knobloch (1996) has described this as a *pitchfork of revolution*, a Hopf bifurcation where the frequency of the bifurcating periodic solution is required to be zero. In phase space, a Hopf bifurcation (which corresponds to a steady wave whose phase may be constant or time-dependent) leads to a limit cycle, while the pitchfork of revolution leads to a continuum of fixed points distinguished only by their spatial phase, ϕ, which, for the case of the two-layer model, may be defined as

$$\phi = \arctan\left(\frac{B_s}{A_s}\right) = \arctan\left(\frac{B_d}{A_d}\right) + \text{constant}. \tag{24}$$

Note that equation (24) is undefined when either A_s and B_s, or A_d and B_d are zero, so that there is only a distinct spatial phase when there is a disturbance on the fluid interface. In a Hopf bifurcation, ϕ varies with time, while ϕ is constant in a pitchfork of revolution.

Numerical integrations performed at $(r, F) = (0.2, 7.0)$ show that the amplitude, $|X| = \sqrt{\left(A_s^2 + B_s^2\right)}$, of the barotropic wave equilibrates to the same value in each layer, whereas ϕ is different. Moreover, after an initial transient, ϕ is constant with time in each case. Together, these results suggest that solutions to the full, complex spectral amplitude equations on an f-plane are distinguished only by their spatial phase.

The pitchfork of revolution arises because of the underlying symmetry group of equations (20). Because the f-plane equations possess $O(2)$ symmetry, the results of the bifurcation analyses performed previously can be generalised to the case where X and Y are complex, simply by multiplying by an arbitrary phase factor. Therefore, the fixed point created in the initial bifurcation in the restricted *real* system (23) actually represents a continuum of fixed points in the full *complex* system (20). By analogy, the limit cycle involved in the Hopf bifurcation at $(r, F) = (0.02, 6.17)$ is actually a continuum of limit cycles distinguished solely by their spatial phase. This continuum of limit cycles forms a torus in phase space, which corresponds to a quasi-periodic or two-frequency, amplitude-modulated travelling wave. Hence, the Hopf bifurcation encountered in the restricted system, where X and Y were real, actually corresponds to a *bifurcation to an invariant torus* in the full complex system. One of the frequencies involved in this torus bifurcation represents the rate of change of ϕ. As has been shown, ϕ is constant on an f-plane and this frequency is therefore zero. This also means that the homoclinic bifurcation (in which the period of oscillation becomes infinite) encountered in the full spectral amplitude equations represents a *torus* becoming homoclinic to the trivial solution, i.e. in which the amplitude of the modulated travelling wave shrinks to zero, giving way to another state. This is in contrast to the situation occurring in the Lorenz equations in which the homoclinic bifurcation represents a simple *limit cycle* becoming homoclinic to the trivial solution.

5 Two-parameter continuations

To investigate the differences in behaviour between the weakly dissipative system and the strongly dissipative system, it was necessary to perform a two-parameter continuation of the bifurcations encountered in the weakly dissipative system. This involved tracing out curves of the bifurcation points encountered in the one-parameter continuations in the weakly dissipative regime, in the (r, F) plane. The curve of pitchfork bifurcations, calculated analytically from the eigenvalues given in equation (22) and Appendix A, is

$$U_d^2 k_n^2 \left(2F - K^2\right) = r^2 K^2 [1 + 2r\epsilon \left(K^2 + F\right) + r^2 \epsilon^2 K^2 \left(K^2 + 2F\right)]. \tag{25}$$

In the absence of horizontal momentum diffusion (i.e. using the Rossby number, ϵ, as an indicator of the strength of the ∇^4 diffusion term and letting $\epsilon \to 0$) this equation simplifies to

$$F = F_{\text{pf}} = \frac{K^2}{2} + \frac{r^2 K^2}{2U_d^2 k_n^2}, \tag{26}$$

which is equivalent to Pedlosky's condition for the stability of a two-layer flow on an f-plane (Pedlosky, 1970), given by equation (13).

AUTO86's two-parameter continuation facility was used to trace out the curves corresponding to the Hopf and homoclinic bifurcations. It should be noted, however, that AUTO86 does not have the capability of calculating the two-parameter continuation of a homoclinic bifurcation directly. Instead, one must use the two-parameter continuation of a periodic orbit of sufficiently high period to approximate the homoclinic bifurcation. This was done by selecting an orbit with a period of $T = 990$ as a proxy for the homoclinic orbit, and following it in the (r, F)-plane.

The curves of the pitchfork, Hopf and homoclinic bifurcations are shown in Figure 9. Also shown are the one-parameter solution continuations performed in Sections 4.2 and 4.3, for the strongly and weakly dissipative systems respectively. Two features immediately become apparent from this figure. The first is the funnel-shaped curve of the bifurcation lines, as r increases. The second is that all the bifurcation lines appear to meet at a point on the inviscid axis, $r = 0$.

5.1 Quantitative boundaries

The first observation, concerning the shape of the bifurcation curves, explains the transition between the strongly and the weakly dissipative behaviour observed in the full spectral amplitude equations. It also explains the apparent discrepancy between the behaviour observed in these two cases. The strongly dissipative multiple-scale approximation is valid only when $r \approx \mathcal{O}(1)$, while the weakly dissipative analysis is valid only when $r \approx \mathcal{O}\left(\mathcal{F}^{\frac{1}{2}}\right)$. At the transition

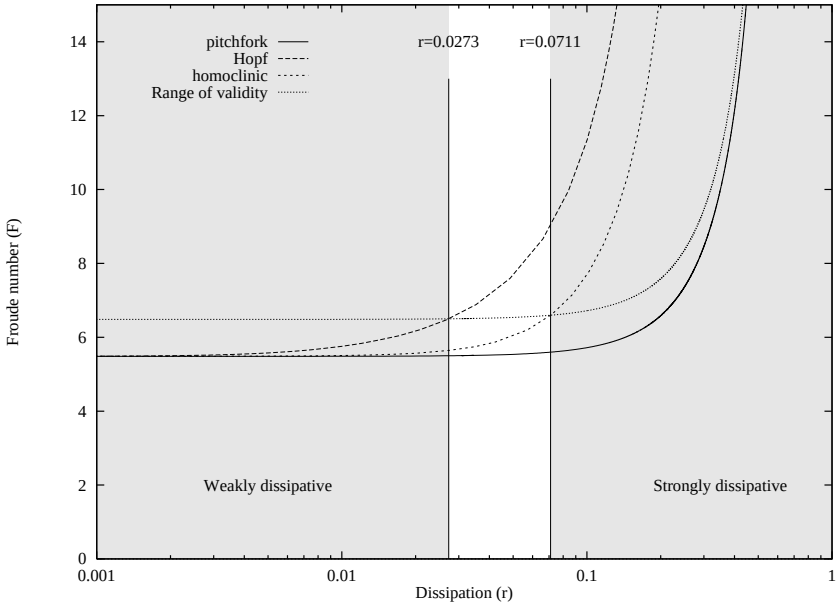

Fig. 9. Two-parameter continuations of the pitchfork, Hopf and homoclinic bifurcations in the $[r, F]$-plane, overlaid with the curve $\mathcal{F} = 1.0$ marking the range of validity of the multiple-scale approximations.

between these two approximations, one might therefore expect $\mathcal{F} \approx 1$. Figure 9 shows the two-parameter continuations for the pitchfork, Hopf and homoclinic bifurcations overlaid with the curve $\mathcal{F} \approx 1$.

As homoclinic bifurcations are not present in the Landau-Stuart equation (the normal form for a Hopf bifurcation) derived for the strongly dissipative multiple-scale system, this approximation is not valid for homoclinic behaviour within the critical region. Conversely, for the weakly dissipative multiple-scale approximation to be valid, both the Hopf and the homoclinic bifurcations must be contained within the critical region. As neither the Hopf nor the homoclinic curves lie within the critical region for $r > 0.07$, one might conclude that the strongly dissipative multiple-scale approximation is valid in this region. Similarly, it would seem that the weakly-dissipative multiple-scale approximation is valid for $0 < r < 0.03$, where both curves lie within the critical region. This observation shows how the strongly dissipative multiple-scale description emerges naturally from the weakly dissipative multiple-scale description as the dissipation parameter is increased: the former is an approximation to the latter. One of the advantages of the spectral amplitude equations can also be seen: their range of validity is not restricted to particular values of the dissipation parameter, r, and so one can capture all the bifurcations present in the one-wave system, regardless of the value of r.

5.2 Bifurcation on the inviscid axis

The second observation, concerning the apparent meeting of the pitchfork, Hopf and homoclinic bifurcation curves on the inviscid axis, is more subtle. Consider the full complex spectral amplitude equations (20) with $r = 0$, so that $\Delta_s = \Delta_d = \bar{\Delta} = 0$ to give

$$\dot{X} = Y + \frac{\gamma_s}{\nu_s} YZ,$$

$$\dot{Y} = \nu_s \nu_d X + \nu_s \gamma_d XZ, \tag{27}$$

$$\dot{Z} = -\frac{\bar{\gamma}}{2\nu_s}\left(XY^* + YX^*\right).$$

As for the dissipative f-plane equations, the trivial solution is always a fixed-point of the equations and its linear stability to small exponentially varying perturbations is determined by the eigenvalues

$$\lambda_{1,2}^2 - \nu_s \nu_d = 0, \quad \lambda_{3,4}^2 - \nu_s \nu_d = 0, \quad \lambda_5 = 0. \tag{28}$$

In contrast to the situation in which $r \neq 0$, one of the eigenvalues, λ_5, is now zero for all values of F, while the real parts of the four remaining complex eigenvalues are all nonzero provided $\nu_s \nu_d \neq 0$. Substituting for ν_s and ν_d from Appendix A, we get

$$U_d^2 k_n^2 \frac{2F - K^2}{2F + K^2} \neq 0. \tag{29}$$

Clearly, (29) is violated when $F = F_c = K^2/2$, where the real parts of the four complex eigenvalues, $\lambda_1 \ldots \lambda_4$, pass through zero simultaneously. F_c is precisely the critical value of the Froude number, derived by Pedlosky (1970), at which an inviscid flow on an f-plane becomes unstable.

6 The organising centre

6.1 Normal form reduction

An analysis of the highly degenerate bifurcation described above is made easier if equations (27) are put into normal form. Guckenheimer and Holmes (1983) and Wiggins (1990) both provide a full account of the theory of normal form calculations. While normal form calculations are straightforward, but tedious to perform manually, the process may

easily be coded up using MAPLE. The calculation of resonant terms, in particular, is easy to implement as the operator, $L_J(\cdot)$, may be written in matrix form. Full advantage of MAPLE's linear algebra routines may then be taken and the calculation of the resonant terms reduces to calculating the left eigenvectors of zero, for $L_J(\cdot)$. Similarly, calculation of the explicit form of the change of variables, described by equation (21), is greatly simplified by using a computer.

6.2 The normal form of the degenerate bifurcation

In order to simplify the calculation of the normal form for the degenerate, inviscid bifurcation, we will once again require the variables x, y and z to be real. The vector field described by the inviscid equations is therefore defined in the space, $\mathbf{R}^3$, which is spanned by the standard vectors

$$\begin{pmatrix}1\\0\\0\end{pmatrix}, \begin{pmatrix}0\\1\\0\end{pmatrix}, \begin{pmatrix}0\\0\\1\end{pmatrix}. \tag{30}$$

In addition, we will simplify the coefficients in the inviscid equations by rewriting equations (27) as

$$\begin{aligned}\dot{x} &= y + ayz,\\ \dot{y} &= bxz,\\ \dot{z} &= cxy,\end{aligned} \tag{31}$$

where

$$a = \gamma_s/\nu_s \ , \quad b = \nu_s\gamma_d \ , \quad c = -\bar{\gamma}/(2\nu_s) \ , \tag{32}$$

so that the normal form, up to fourth order, is

$$\begin{aligned}\dot{x} &= y,\\ \dot{y} &= bxz + \frac{bc}{2}x^3 - \frac{2bac}{3}x^3z - ba^2xz^3,\\ \dot{z} &= 0,\end{aligned} \tag{33}$$

which is structurally unstable to perturbations (see e.g. Guckenheimer and Holmes, 1983, for a discussion of structural stability). The addition of an x^2-term to the $\dot{z}$-equation, for example, will certainly change the behaviour of the system. In order to examine the consequences of such small perturbations, it is necessary to consider an unfolding of the normal form by adding parameter-dependent perturbations. For such a highly degenerate bifurcation, the construction of a universal unfolding can be difficult. Here we discuss one possible unfolding in which only perturbations which influence the $O(2)$ symmetry of the original system are included. This unfolding, however, will not be universal.

6.3 An unfolding of the degenerate bifurcation

Wiggins (1990) showed that, for a vector field in which all resonant terms are present, the universal unfolding of a non-hyperbolic point with Jacobian J is given by $J + B$, where B is a matrix satisfying

$$\left[B^*, J\right] = 0, \tag{34}$$

and * denotes the adjoint of B. For a non-hyperbolic point

$$J = \begin{pmatrix}0&1&0\\0&0&0\\0&0&0\end{pmatrix}, \tag{35}$$

and

$$B = \begin{pmatrix}0&0&0\\\mu_1&\mu_2&\mu_3\\\mu_4&0&\mu_5\end{pmatrix}, \tag{36}$$

where $\{\mu_1, \mu_2, \mu_3, \mu_4, \mu_5\} \in \mathbf{R}$, so that the unfolding is given by

$$\begin{pmatrix}0&1&0\\\mu_1&\mu_2&\mu_3\\\mu_4&0&\mu_5\end{pmatrix}. \tag{37}$$

Inclusion of μ_3 and μ_4 would, however, violate the reflection symmetry ρ, defined in equations (18). A more suitable candidate for a universal unfolding which preserves the original symmetry of the system is therefore

$$\begin{pmatrix}0&1&0\\\mu_1&\mu_2&0\\0&0&\mu_5\end{pmatrix}, \tag{38}$$

and the normal form equations then become

$$\begin{aligned}\dot{x} &= y,\\ \dot{y} &= \mu_1x + \mu_2y + bxz + \frac{bc}{2}x^3 - \frac{2bac}{3}x^3z\\ &\quad - ba^2xz^3,\\ \dot{z} &= \mu_5z.\end{aligned} \tag{39}$$

Wiggins' approach assumed that no crucial resonant terms were "missing" from the normal form. This is not the case here, since a straightforward calculation shows that x^2 and xz are both resonant in the $\dot{z}$-equation. The inclusion of these terms, as additional perturbations to equation (39), may therefore be warranted. The case for the inclusion of a second-order term in the $\dot{z}$-equation is further strengthened by noting that the full spectral amplitude equations (20), include xy in the $\dot{z}$-equation. Here, only the x^2 term will be included in the $\dot{z}$-equation. A more general analysis, however, might include the xz term as well.

We therefore investigate the unfolding of

$$\begin{aligned}\dot{x} &= y,\\ \dot{y} &= \mu_1x + \mu_2y + bxz + \frac{bc}{2}x^3 - \frac{2bac}{3}x^3z\\ &\quad - ba^2xz^3,\\ \dot{z} &= \mu_5z + \mu_6x^2.\end{aligned} \tag{40}$$

To third order, this unfolding is identical to a form of the Lorenz equations considered by Rychlik (1990) (see also Robinson, 1989). Rychlik used this form to prove that the Lorenz equations contain a strange attractor. This unfolding means that close to the inviscid bifurcation, where terms of fourth and higher order are small enough to be ignored, perturbations to the inviscid bifurcation in the spectral amplitude

equations can give rise to Lorenz-like behaviour. This places a more formal limit (that r must be small enough to allow the fourth-order terms in the normal form expansion to be neglected) on the range of r for which the weakly dissipative multiple-scale approximation is valid.

When the dissipation parameter is larger, the fourth-order terms in equation (40) cannot be neglected. Note that all of these fourth order terms contain the coefficient a, which is the coefficient of the non-resonant yz term in the $\dot{x}$ component of the spectral amplitude equations (20). This implies that if this term were absent, the spectral amplitude equations would be exactly equivalent to the Lorenz equations and therefore to the weakly-dissipative multiple-scale equations derived by Pedlosky. The presence of this yz term is therefore a crucial difference between the spectral amplitude equations and the weakly-dissipative multiple-scale equations.

As r increases, the fourth-order terms in the unfolding become important and consequently the yz term becomes more important to the dynamics of the system. This means that the interaction between the baroclinic wave, y, and the mean-flow correction, z, becomes more important in supplying energy to the barotropic wave, x, and may be regarded as a physical explanation for the differences in the behaviour of strongly and weakly dissipative systems.

Recall that, in constructing the unfolding (40), x and y were assumed to be real. In addition, this unfolding was constructed to preserve the $O(2)$ symmetry of the system. As has been shown previously, this implies that the behaviour deduced above still holds for the case when x and y are complex. The analytical construction of an unfolding that breaks the $O(2)$ symmetry of the system is more difficult and is outside the scope of the present study. In Part II, however, numerical methods will be used to examine the effects of breaking this symmetry by including a β-effect.

7 Derivation of the inviscid multiple-scale equations

The connection between the spectral amplitude equations and the strongly and weakly dissipative multiple-scale approximations on an f-plane has been shown. The relation between the spectral amplitude equations and the f-plane, inviscid multiple-scale approximation of Pedlosky (1970), given in equation (15) has not, so far, been established. Consider the unfolding of the inviscid normal form, truncated at third order:

$$\begin{aligned}\dot{x} &= y,\\ \dot{y} &= \mu_1 x + \mu_2 y + bxz + \frac{bc}{2}x^3,\\ \dot{z} &= \mu_5 z + \mu_6 x^2.\end{aligned} \tag{41}$$

Setting the unfolding parameters μ_2, μ_5 and μ_6 to zero, and making the change of variables $z \rightarrow -z - \frac{c}{2}x^2$, the normal form now becomes

$$\begin{aligned}\dot{x} &= y,\\ \dot{y} &= \mu_1 x - bxz,\\ \dot{z} &= -cxy,\end{aligned} \tag{42}$$

representing a small perturbation to the inviscid bifurcation. Eliminating y gives

$$\begin{aligned}\ddot{x} &= \mu_1 x - bxz,\\ \dot{z} &= -\frac{c}{2}\dot{(x^2)},\end{aligned} \tag{43}$$

which is the equivalent of equation (15), derived by Pedlosky (1970).

8 Discussion

In this paper, the spectral amplitude equations for the two-layer f-plane model were used to examine the differences between the multiple-scale approximations of Pedlosky (1970, 1971) for different dissipative regimes. This was possible because the derivation of the spectral amplitude equations does not require any restriction to be placed on the size of the dissipation parameter, r, thereby giving the spectral amplitude equations validity over the range $0 \leq r \leq 1$. The spectral amplitude equations were shown to reproduce the behaviour observed in both the strongly and the weakly dissipative multiple-scale approximation when the spectral variables x and y were restricted to being real. It was then shown that, because the full complex spectral amplitude equations were equivariant under the action of the $O(2)$-symmetry group, the results from the real system could be generalised to the complex case.

In addition, it was shown that the strongly dissipative multiple-scales approximation arises naturally from the weakly dissipative multiple-scale equations. Also, a quantitative criterion for deciding when the strongly dissipative approximation holds was found to be $r > 0.07$, while the weakly dissipative approximation is valid for $0 < r < 0.03$.

The bifurcations present in the weakly dissipative limit were shown to originate in a degenerate bifurcation on the inviscid axis and, close to this degenerate bifurcation, fourth-order terms in the normal form expansion of the inviscid spectral equations may be ignored. Small $O(2)$-symmetry-preserving perturbations to this third-order normal form then give rise to the Lorenz equations, producing the dynamics associated with the weakly dissipative multiple-scale approximation. Further away from this degenerate bifurcation, fourth-order terms in the normal form expansion become important. This corresponds to the transition from weakly to strongly dissipative behaviour. A subset of the symmetry-preserving perturbations was then shown to produce the equations discovered by Pedlosky (1970).

In contrast to the earlier study of Klein and Pedlosky (1992), who found that the inclusion of interfacial Ekman layers or potential vorticity damping tended to suppress amplitude vacillations and chaotic dynamics, the inclusion here of ∇^4 internal friction does not suppress chaotic behaviour. In some respects, this parallels the results of Mundt et al.

(1995), who found that viscous $E^{1/4}$ sidewall boundary layers were instrumental in causing a transition to baroclinic chaos.

In Part II we reinstate the β-effect and explore the resulting changes to the bifurcation scenarios when $\beta \neq 0$.

Appendix A Coefficients of the Single-wave model

The coefficients to equations (9) and (20) are:

$$K^2 = k_1^2 + l_1^2 \tag{A1}$$

$$\Delta_s = r\left[1 + r\epsilon K^2\right] \tag{A2}$$

$$\Delta_d = \frac{rK^2}{\left(K^2+2F\right)}\left[1 + r\epsilon\left(K^2+2F\right)\right] \tag{A3}$$

$$\bar{\Delta} = \frac{rl_1^2}{\left(l_1^2+2F\right)}\left[1 + r\epsilon\left(l_1^2+2F\right)\right] \tag{A4}$$

$$\beta_s = \left[\frac{\beta}{K^2} - U_s\right]k_1 \tag{A5}$$

$$\beta_d = \left[\frac{\beta}{\left(K^2+2F\right)} - U_s\right]k_1 \tag{A6}$$

$$v_s = U_d k_1 \tag{A7}$$

$$v_d = U_d\frac{\left(K^2-2F\right)}{\left(K^2+2F\right)}k_1 \tag{A8}$$

$$\gamma_s = \frac{16{k_1}^3}{6K^2} \tag{A9}$$

$$\gamma_d = \frac{16k_1\left(k_1^2-2F\right)}{6\left(K^2+2F\right)} \tag{A10}$$

$$\bar{\gamma} = \frac{32Fk_1}{3\left(l_1^2+2F\right)} \tag{A11}$$

Acknowledgements. AFL acknowledges support under a research studentship from the UK Engineering and Physical Sciences Research Council and Smiths System Engineering.

References

Appleby, J. C., Comparative theoretical and experimental studies of baroclinic waves in a two-layer system, Ph.D. thesis, University of Leeds, 1982.

Booty, M., Gibbon, J. D., and Fowler, A. C., A study of the effect of mode truncation on an exact periodic solution of an infinite set of Lorenz equations, Phys. Lett., 87A, 261–266, 1982.

Curry, J. H., A generalised Lorenz system, Commun. math. Phys., 60, 193–204, 1978.

Doedel, E., Auto: a program for the automatic bifurcation analysis of autonomous systems, Cong. Numer., 30, 265–284, 1981.

Doedel, E. J. and Kernevez, J. P., Auto: software for continuation and bifurcation problems in ordinary differential equations, Tech. rep., Applied Mathematics Report, California Institute of Technology, 1986.

Früh, W.-G. and Read, P. L., Wave interactions and the transition to chaos of baroclinic waves in a thermally driven rotating annulus, Phil. Trans. Roy. Soc. Lond, 355, 101–153, 1997.

Gibbon, J. D. and McGuinness, M. J., The real and complex Lorenz equations in rotating fluids and lasers, Physica D, 5, 108–122, 1982.

Guckenheimer, J. and Holmes, P. J., Nonlinear Oscillations, Dynamical Systems, and Bifurcations of Vector Fields, Springer-Verlag, New York, 1983.

Hart, J. E., Finite amplitude baroclinic instability, Ann. Rev. Fluid Mech., 11, 147–172, 1979.

Hart, J. E., A model for the transitions to baroclinic chaos, Physica D, 20, 350–362, 1986.

Hide, R. and Mason, P. J., Sloping convection in a rotating fluid, Advances in Physics, 24, 47–99, 1975.

James, I. N., Stability of a slowly rotating two-layer system, Occasional Note Met. O. 21/77/2, UK Met. Office, 1977.

King, J. C., An experimental study of baroclinic wave interactions in a two-layer system, Geophys. Astrophys. Fluid Dyn., 13, 153–167, 1979.

Klein, P., Transitions to chaos in unstable baroclinic systems: a review, Fluid Dyn. Res., 5, 235–254, 1990.

Klein, P. and Pedlosky, J., A numerical study of baroclinic instability at large supercriticality, J. Atmos. Sci., 43, 1243–1262, 1986.

Klein, P. and Pedlosky, J., The role of dissipation mechanisms in the nonlinear dynamics of unstable baroclinic waves, J. Atmos. Sci., 49, 29–48, 1992.

Knobloch, E., Symmetry and instability in rotating hydrodynamic and magnetohydrodynamic flows, Phys. Fluids, 8, 1446–1454, 1996.

Lewis, S. R., A quasi-geostrophic numerical model of a rotating internally heated fluid, Geophys. Astrophys. Fluid Dyn., 65, 31–55, 1992.

Lorenz, E. N., Simplified dynamic equations applied to the rotating basin experiment, J. Atmos. Sci., 19, 39–51, 1962.

Lorenz, E. N., Deterministic nonperiodic flow, J. Atmos. Sci., 20, 130–141, 1963.

Lovegrove, A. F. L., Bifurcations and instabilities in rotating two-layer fluids, Ph.D. thesis, University of Oxford, 1998.

Moroz, I. M., Slowly varying baroclinic waves in dispersive and dissipative systems, Ph.D. thesis, Leeds, 1981.

Mundt, M. D., Hart, J., E., and Ohlsen, D., R., Symmetry, sidewalls, and the transition to chaos in baroclinic systems, J. Fluid Mech., 300, 311–338, 1995.

Pedlosky, J., Finite-amplitude baroclinic waves, J. Atmos. Sci., 27, 15–30, 1970.

Pedlosky, J., Finite-amplitude baroclinic waves with small dissipation, J. Atmos. Sci., 28, 587–597, 1971.

Pedlosky, J., Geophysical Fluid Dynamics, Springer-Verlag, Berlin, 1987.

Pedlosky, J. and Frenzen, C., Chaotic and periodic behaviour of finite-amplitude baroclinic waves, J. Atmos. Sci., 37, 1177–1196, 1980.

Phillips, N. A., Energy transformations and meridional circulations associated with simple baroclinic waves in a two-level quasi-geostrophic model, Tellus, 6, 273–286, 1954.

Polvani, L. M. and Pedlosky, J., The effect of dissipation on spatially growing nonlinear baroclinic waves, J. Atmos. Sci., 45, 1977–1989, 1988.

Read, P. L., Bell, M. J., Johnson, D. W., and Small, R. M., Quasi-periodic and chaotic flow regimes in a thermally-driven, rotating fluid annulus, J. Fluid Mech., 238, 599–632, 1992.

Robinson, C., Homoclinic bifurcation to a transitive attractor of Lorenz type, Nonlinearity, 2, 495–518, 1989.

Rychlik, M. R., Lorenz attractors through Silnikov-type bifurcation, part I, Ergodic Theor. Dyn. Syst., 10, 793–821, 1990.

Sparrow, C., The Lorenz Equations, Springer-Verlag, New York, 1982.

Wiggins, S., Introduction to applied nonlinear dynamical systems and chaos, Springer-Verlag, New York, 1990.